Experimental limit for the charge of the free neutron

R. Gähler
Universität Bayreuth, 858 Bayreuth, Germany
and Institut Laue-Langevin, 38042 Grenoble, France

J. Kalus
Universität Bayreuth, 858 Bayreuth, Germany

W. Mampe
Institut Laue-Langevin, 38042 Grenoble, France

(Received 15 April 1981)

The neutron charge has been measured to be $q_n = (-1.5 \pm 2.2) \times 10^{-20}$ electron charges at a confidence level of 90%. This value lowers the known limit by two orders of magnitude. In the experiment, slow neutrons of 20-Å wavelength passed a strong electric field of 10-m length. The deflection of the neutron beam was measured with respect to reversal of the field. For an increase in sensitivity the beam was focused by a neutron lens to a sharp image in the detector plane. Over a long run time the deflection of the neutron beam due to the electric field was less than 2×10^{-2} μm. The result on the neutron charge is in agreement with the commonly accepted neutrality of the neutron. The implications of a hypothetical neutron charge are discussed and an improved apparatus is proposed which could lower the limit on the free neutron's charge by up to two orders of magnitude.

INTRODUCTION

Within the framework of modern unified theories even a tiny electric charge of the neutron q_n would lead to important consequences: Assuming charge conservation, a finite neutron charge implies that a transition neutron-antineutron, as predicted by some theories,[1] is not allowed; the electric charge has to change its sign in such a transition. Furthermore, if it were found that all baryons have charges slightly displaced from their usually accepted values by a common amount ϵ, then the conservation of baryons would follow from the conservation of electric charge rather than being an independent principle.[2] In this case the decay of the proton, predicted by several unified theories, is forbidden because the leptons into which it could decay carry a different charge.

With the present measurement, a new experimental limit for the charge of the electron neutrino $q_{\bar{\nu}}$ can be set by considering the β decay of the neutron

$$n \rightarrow p + e + \bar{\nu} \ .$$

The neutrality of the system proton-electron, i.e., the neutrality of the hydrogen atom, has been measured to $(0.9 \pm 2.7) \times 10^{-21} \times q_e$ (q_e = charge of the electron).[3] Combined with the new value for the neutron charge, one gets

$$q_{\bar{\nu}} = (1.4 \pm 1.4) \times 10^{-20} \times q_e \ \ (68\% \text{ confidence}) \ .$$

For these considerations charge conservation has been assumed to be valid.

Whereas newer theories assume the symmetry of the existing electric charges (this implies $q_n = 0$), there have been some theories in the past predicting a finite neutron charge. The observed expansion of the universe would follow from a neutron charge of about $2 \times 10^{-18} \times q_e$,[4] and the Earth's magnetic field was explained by a neutron charge of about 2×10^{-19} electron charges.[5] These theories can be refuted by our measurement.

I. EARLIER MEASUREMENTS

Most experimental limits on the neutron charge have been derived in an indirect way by testing the charge neutrality of atoms or macroscopic bodies. For a review of these experiments see Dylla and King.[3] We have only to add more recent measurements, which dealt with the search for fractional charges in matter.[6-9] The sensitivity of all these measurements is in the region of 10^{-21} to 10^{-23} electron charges for the sum of $q_e + q_p + q_n$.

Direct measurements on the charge of the free neutron are all based on the deflection of a neutron beam in a strong homogeneous electric field. In the latest and most precise experiment of this type Shull *et al.*[10] obtained a limit on the neutron charge of $q_n = (-1.9 \pm 3.7) \times 10^{-18} \times q_e$. In that experiment not the lateral deflection of the neutron beam was sensed, but its angular deviation, using perfect Si crystals in Bragg condition. The authors also review all earlier charge measurements on the free neutron. It should be noted that the sensitivity of all direct measurements including ours is lower than that of indirect methods. But

as mentioned by Shull *et al.*,[10] "the possibility of a free charge being slightly different in magnitude, at this small level of charge difference when particles are amalgamated into an atom, does exist."

II. MEASURING PRINCIPLE

In the reported experiment a beam of slow neutrons (velocity $v=200$ m/sec, wavelength $\lambda=20$ Å) enters through a narrow slit S_3 into a strong transverse electric field of about 10-m length (see Fig. 1). A neutron charge q_n would lead to a deflection of the beam correlated to the direction of the periodically reversed electric field. The deflection y is given by

$$y=\frac{q_n E_0 l^2}{4Q_0} \tag{1}$$

(see Sec. III) with E_0 the electric field applied over the length l and Q_0 the kinetic energy of the neutron. After passage through the electric field the neutrons are counted behind slit S_4, which is positioned in the slope of the neutron beam image. A change in count rate for opposite field directions would indicate a beam deflection and hence a charge of the neutron. The sensitivity for measuring a deflection depends on the steepness of the slope and on the intensity. In order to obtain a narrow beam with high intensity, we studied different focusing systems and found a lens to be the most convenient device.[11] Similar to a lens in light optics, this neutron lens relies on the difference of the indices of refraction in the lens material and in air. The severely chromatic lens (focal length $f\sim 1/\lambda^2$) requires a fairly monochromatic beam. This is obtained by a prism monochromator in front of slit S_3. The neutron lens is positioned 5 m downstream from the entrance slit S_3, which is 40 μm wide. The lens images the slit S_3 onto a plane where slit S_4 is positioned. A detailed description of the optical system has been given in a previous paper.[11]

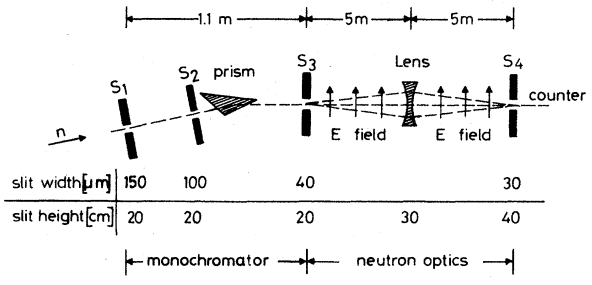

FIG. 1. Top view of the instrument (not to scale).

III. SENSITIVITY FOR THE CHARGE MEASUREMENT

A. Deflection of a charge q_n in the electric field

First it will be shown that for our optical system the beam deflection is only half that without imaging by the lens.

In WKB approximation, the deflection y is derived in the following way (see Fig. 2). We consider the neutron waves along two paths a and b which are symmetric to the optical axis. The mean electric potentials for these paths are different. This implies for $q_n\neq 0$ different optical path lengths and thus the point of constructive superposition for both waves is shifted. For the following the electric field is assumed to fill the whole region between S_3 and S_4. The energy Q_E of a charge q_n in the electric potential U relative to a point where U is zero is given by

$$Q_E=q_n U\ . \tag{2}$$

The index of refraction n becomes

$$n=1-\frac{q_n U}{2Q_0}\quad (q_n U\ll Q_0)\ , \tag{3}$$

where Q_0 is the kinetic energy of the neutron at $U=0$. This leads to an optical-path difference Δl:

$$\Delta l=\int_{\text{path }a}(n_a-1)dl_a-\int_{\text{path }b}(n_b-1)dl_b\ . \tag{4}$$

With $n-1$ from (3) and $U_a-U_b=2xE_0$ (see Fig. 2) we get

$$\Delta l=\frac{q_n E_0}{2Q_0}\,x_0 l_0 \tag{5}$$

with x_0 shown in Fig. 2. The resulting shift of the image y—the shift of the point for which the optical paths a and b are equal—is derived by a simple geometrical construction which leads to

$$\frac{y}{l_0}=\frac{\Delta l}{4x_0}\ . \tag{6}$$

Together with (5) the deflection y becomes

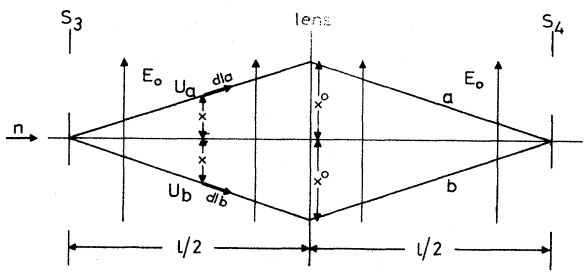

FIG. 2. Beam deflection in a wave-optical treatment.

$$y=\frac{q_n E_0 l_0^2}{8Q_0} . \tag{7}$$

This shows [by comparison with (1)] that for our optical device with magnification 1, the beam deflection y is only half the value compared to a beam which travels freely over the same length. Using geometrical optics, one gets the same formula for the deflection y. A neutron starting parallel to the optical axis follows a parabola in the E field leading to a deflection $y/4$. Owing to the focusing properties of the lens, the flight path is bent back parallel to the optical axis. The E field downstream from the lens bends the flight-path to an identical parabola as before, leading to an additional deflection $y/4$. The loss factor of 2 could be compensated by increasing the image distance relative to the object distance. But in this case the required precision for the lens—already a delicate problem—becomes even more severe.

In our case the electric field E_0 is not applied over the full length l_0 between S_3 and S_4—the necessary control of the optical components implied the need to divide the field into two halves, one between S_3 and the lens, and the other between the lens and S_4. If the total length of the electric field is l_1, it can simply be shown that the deflection y becomes

$$y=\frac{q_n E_0 l_0 l_1}{8Q_0} . \tag{8}$$

This is valid if the two electric fields are arranged symmetrically with respect to the optical elements. With the given parameters of the machine the deflection y for a hypothetical charge of $q_n = 1\times10^{-20}\times q_e$ becomes

$$y=6.5\times10^{-9}\ \text{m}$$

$[E_0=11.9\times10^6\ \text{V/m},\ l_0=10\ \text{m},\ l_1=9\ \text{m},\ Q_0 = 2\times10^{-4}\ \text{eV}\ (\lambda=20\ \text{Å})]$.

B. Choice of the instrumental parameters

The parameters which determine the sensitivity of the apparatus for the charge measurement are the count rate N at slit S_4, the width of the image w_0, the wavelength λ (energy Q_0), the lengths l_0 and l_1, and the electric field E_0. The actual values of these parameters will be discussed now.

1. Count rate N and width of the image w_0

The statistical error σ_N of the difference in count rate N_1-N_2 for the two different directions of E_0 is given by

$$\sigma_N=(2N)^{1/2} \tag{9}$$

for $N_1\approx N_2=N$ and negligible background. The measurable shift σ_y of the image is given by

$$\sigma_y=\frac{\sigma_N}{dN/dy} , \tag{10}$$

where dN is the change in count rate per shift dy and

$$\frac{dN}{dy}=N\frac{df}{dy} \tag{11}$$

with df/dy being the steepness of the slope of the image at the position of slit S_4. It follows that

$$\sigma_y=\frac{\sqrt{2}}{\sqrt{N}\,df/dy} . \tag{12}$$

In the first approximation the image has Gaussian shape. At the steepest point of the slope, $1/(df/dy)$ is proportional to w_0, the width of the image, and

$$\sigma_y\sim\frac{w_0}{\sqrt{N}} . \tag{13}$$

In order to minimize σ_y, a small image width w_0 with a high count rate N is desired. The count rate N increases with the width of the wavelength band and with the beam divergence. However, imperfections and aberrations of the focusing lens limit the achievable σ_y. A good compromise between high count rate N and small image width w_0 is obtained using the following argument: The parallelism of the four axes of the lens system (see Ref. 11) is about 10 μm. At the position of the image this leads to a broadening of about 20 μm for each point of the object, the slit S_3. It follows that a slit width smaller than about 40 μm is not useful for S_3. Further broadening of the image arises from the spherical and chromatic aberration. A broadening of each point to about 30 μm was accepted for each of the two aberrations. Concerning the spherical aberration, this allows a beam width of about 1.5 mm in the plane of the lens. For the chromatic aberration we obtain an acceptable wavelength band of $\Delta\lambda=\pm0.3$ Å at a mean wavelength of 20 Å. In reality a wider wavelength band of $\Delta\lambda=\pm0.5$ Å can be accepted because of the following reason: The monochromator in front of slit S_3 (see Fig. 1) delivers a neutron-spectrum which is asymmetric over the beam cross section because the deflection angle of the prism is proportional to λ^2. Therefore, by underfocusing the shorter and overfocusing the longer wavelengths, one slope of the image is broadened, the other becomes steeper (see Fig. 3). Only the steeper slope was used for the charge measurement.

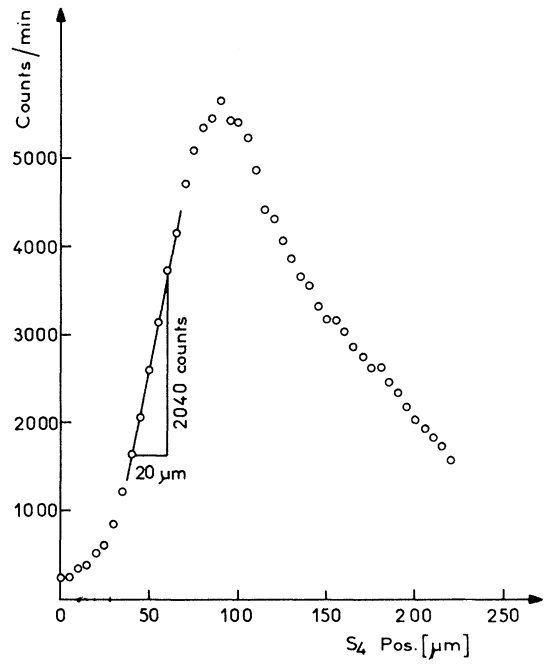

FIG. 3. Image of slit S_3 in the plane of slit S_4. The steeper slope was taken for the charge measurement.

The steeper slope corresponds to a width of the image of about 80 μm. The width of slit S_4 was taken as 40 μm for optimal sensitivity. The count rate behind S_4 is about 50 n/sec.

2. *Mean wavelength* λ_0

The sensitivity of the apparatus to detect a neutron charge q_n is independent of the choice of the mean wavelength λ_0, as long as cold neutrons are used. This is due to the chromatism of the neutron lens and due to the reactor spectrum.

The reactor spectrum $d\phi/d\lambda$ varies as λ^{-5} for cold neutrons. Integrated over $d\lambda$—the wavelength band accepted by the lens—we get $\phi \sim d\lambda/\lambda_0^5$. The focal length f of the lens is proportional to $1/\lambda_0^2$. It follows that $df/f \sim d\lambda/\lambda_0$. Thus, for constant focal length f and constant acceptable width df resulting from chromatic aberration, the value $d\lambda/\lambda_0$ is constant. Therefore, the usable intensity becomes proportional to $1/\lambda_0^4$. The deflection of a possible charge q_n in the E field is proportional to λ_0^2 and we get with (13) for σ_{q_n}, the precision for the measurement of a neutron charge

$$\sigma_{q_n} \sim \frac{w_0}{\lambda_0^2\sqrt{N}} . \tag{14}$$

Since, as shown above, the count rate is proportional to λ_0^{-4}, σ_{q_n} becomes independent of λ_0. The spectrum of the guide H18 is peaked at 20 Å with a width of about 10 Å. Shorter wavelengths are cut off because of the curvature of the guide. A mean wavelength of 20 Å was selected from the monochromator because the high intensity simplifies the alignment of the optical components. The mean wavelength and the wavelength spread of ± 0.5 Å selected by the monochromator was checked using the critical angle of total reflection from a Ni mirror. During the charge measurement the mean wavelength was controlled by the width of the image. This control was possible because of the severe chromatism of the lens.

3. *Lengths* l_0, l_1

The length l_0 of the apparatus was limited by the available space inside the reactor hall of the Institut Laue-Langevin (ILL). The best suited area was that at the neutron guide H18, where a free length of 13 m was available.

4. *Electric field*

The total length of the electric field was 9 m. It reached from the entrance slit S_3 to slit S_4 in front of the detector and was separated by the lens into two sections of equal length. The beam height of the divergent neutron beam increased from 0.2 m at slit S_3 to about 0.38 m at slit S_4. This leads to rather large dimensions of the electrodes: The first one has an area of 0.32×4.5 m, the second one 0.4×4.5 m. For reasons of high electric field and for mechanical stability each electrode was a stainless-steel tube with rectangular cross section. The surfaces which produce the electric field were milled. The waviness of each surface was about 0.1 mm, thus being significantly lower than the 2.5-mm gap between the electrodes. The mean gap between the electrodes which determines the mean electric field E_0 was measured with a capacity meter. One electrode of each pair was connected to ground and the other one to a high-voltage (HV) supply with a maximum output of 30 kV at 2 mA. Each pair of electrodes was mounted inside a vacuum tube of 0.8-m diameter and 4.6-m length. A vacuum of better than 10^{-4} Torr was maintained in each tube by a turbomolecular pump. The tubes were supported independently from the optical bench and thus mechanically decoupled from the neutron optical system.

The charge measurement was performed with an electric field of ± 5.9 kV/mm. The field was limited to this value by voltage breakdown due to imperfect finishing and cleanliness of the elec-

trode surfaces. Attempts at more efficient cleaning by glow discharging had to be abandoned because of damage to the insulators. Teflon had been chosen as insulator material because of its shock absorbing qualities in the case of high-voltage breakdowns.

IV. MEASUREMENTS AND RESULTS

A. Performance of the measurement

At the beginning of each cycle the high voltage was raised in about 1 sec to its nominal value; after a waiting time of 2 sec the measurement, lasting 10 sec, was started. The count rate was recorded on magnetic tape and the high voltage was switched off. Then a measurement with reversed electric field was started. About 1000 to 3000 such cycles were combined to form one run. At the end of such a run we regularly checked the steepness of the slope of the image in order to be sure that the sensitivity had not changed. The BF_3 detector was connected to two scalers, one for each polarity of the high voltage. Two monitor counters were used, one for monitoring the incoming flux in front of slit S_1 and one near slit S_4 in order to detect changes in background. In the case of a high-voltage breakdown (about one in 5 minutes) the measurement was stopped and the actual count rate was deleted.

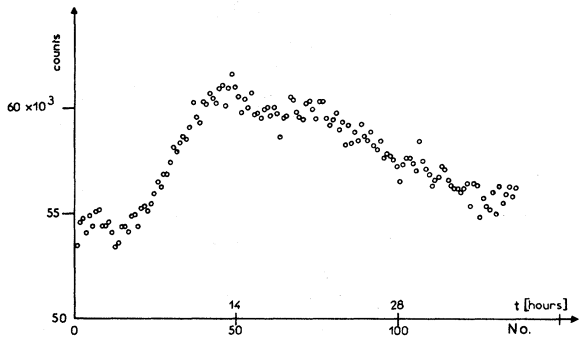

FIG. 4. Drift of the count rate during one run at a position of maximum slope. Each point combines the count rate of 20 cycles.

B. Data analysis

Each of the 54 runs was analyzed separately. We observed a change of the count rate of less than ± 10% within one run, corresponding to a drift of the image of less than ±5 μm (see Fig. 4). This drift is probably due to thermal effects, though the reactor hall is temperature stabilized (within ± 1 °C). This drift was small enough to take the slope dN/dy as constant. The difference in count rate for the two field directions ΔN was compared to the square root of the count rate $\sqrt{N}$. These values for all runs are shown in Fig. 5, calculated in terms of the neutron charge. A

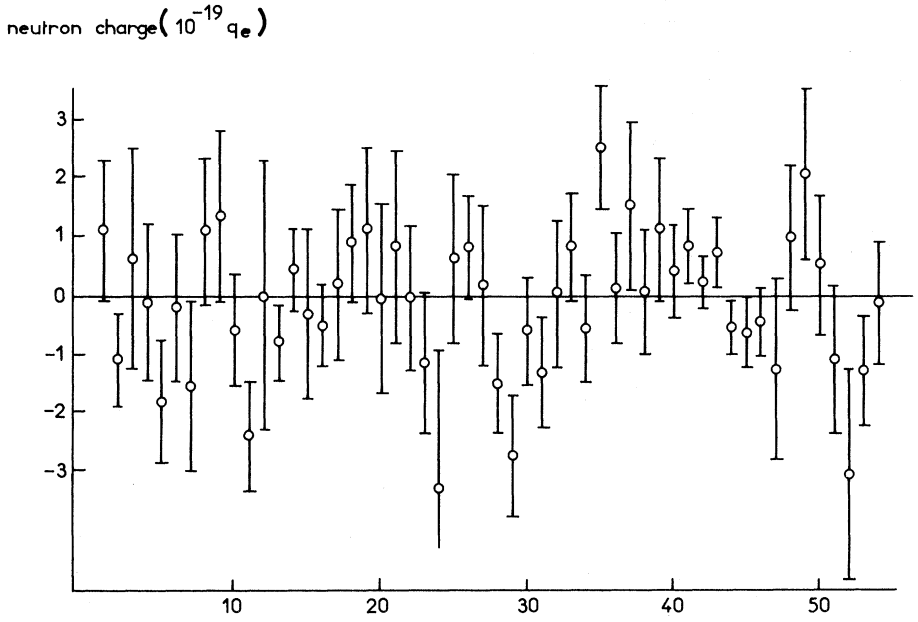

FIG. 5. Electric charge of the neutron for each run.

χ^2 test was made for ΔZ, the difference in count rate for every measurement cycle, i.e., each pair of count rates with opposite field ($\Delta Z = Z_+ - Z_-$), assuming $\Delta Z = 0$ as expectation value. For each run the value of $f(\chi^2) = (2\chi^2)^{1/2} - (2A-1)^{1/2}$ (Ref. 12) (A = number of cycles per run) was calculated. Considering only statistical errors (and no systematic shift of the image), the distribution of the values $f(\chi^2)$ should be a Gaussian centered at zero with a standard deviation of 1. The agreement with these expectation values was good; we obtained a mean χ^2 per run of $\chi^2 = 1.02$. This indicates that systematic errors are small compared to the statistical errors.

A second χ^2 test, performed with the results from all runs (Fig. 5), delivers a χ^2 of 1.2. Consequently the error bars from all runs were increased (not shown in Fig. 5), in order to obtain a value of 1.0 for χ^2.

The errors from the determination of the mean wavelength λ, the length l, and the electric field E can be neglected. We obtain as a final result

$$q_n = (1.5 \pm 1.4) \times 10^{-20} \times q_e \quad (68\% \text{ confidence}),$$
$$q_n = (1.5 \pm 2.2) \times 10^{-20} \times q_e \quad (90\% \text{ confidence}).$$

C. Test measurements

To test whether the apparatus produces a difference in count rate which is not due to the interaction of a hypothetical charge q_n with the electric field, we performed two other types of measurements.

(1) Seven runs were taken with high electric field E_0 for one direction but zero for the other. This test was done for the following reason: The electrostatic attraction of the electrodes changes the gap between them (the change was less than 20 μm). Neutrons striking the electrodes are reflected and can contribute to the count rate behind slit S_4. If the E field were not exactly the same for both directions ($|E_+| - |E_-| < 10^{-3} \times E_+$), the reflected intensities might be different for both directions of E. This could produce a misleading shift of the image. The measurement with zero field in one direction increases this possible effect by about three orders of magnitude. For these test measurements, we obtained, calculated in terms of the neutron charge,

$$q_n = (0.1 \pm 4.6) \times 10^{-20} \times q_e .$$

Therefore, this effect can be neglected for the charge measurement. The results with zero field in one direction were used together with the other charge measurements to obtain the final value.

(2) Eight long runs were performed without any electric field. The measured deflection of the image was

$$y = (-0.8 \pm 1.3) \times 10^{-2} \mu\text{m},$$

assuming negligible systematic errors. This result indicates that there is no significant beam deflection simulated by possible errors in the counting system. For comparison the deflection from the measurements with electric field was

$$y = (9.8 \pm 8.9) \times 10^{-3} \mu\text{m},$$

including systematic errors.

V. SYSTEMATIC ERRORS DUE TO THE ELECTRIC FIELD

Besides a possible charge q_n, the magnetic moment of the neutron and its inner structure can give rise to a deflection of the neutron in an electric field. It is not possible to separate these forces experimentally from the force acting on a neutron charge because most of them are coupled to the direction of E. In this section it will be shown that the deflection caused by a neutron charge of $q_n = 1 \times 10^{-20} \times q_e$—the sensitivity of the reported measurement—is large compared to all other deflections. The most convenient way is the wave-optical treatment used for the calculation of the deflection of a charge q_n (Sec. III). It will be shown in the Appendix that ΔQ, the mean energy difference between the symmetric paths a and b is much smaller for all competing effects than that resulting from a charge $q_n = 1 \times 10^{-20} \times q_e$. The energy Q of a neutron in an electromagnetic field is given by[13]

$$Q = q_n U + \vec{\mu}_n \cdot \vec{H} + \vec{\mu}_n \cdot \epsilon_0 \vec{E} \times \vec{v} + \frac{h \mu_n E_0}{2m} \vec{\nabla} \cdot \vec{E} + C_1 E + \tfrac{1}{2} C_2 E^2 + \vec{p} \cdot \vec{E}$$
$$= \text{I} + \text{II} + \text{III} + \text{IV} + \text{V} + \text{VI} + \text{VII},$$

where

I is energy of charge q_n in a potential U,

II is energy of magnetic moment $\vec{\mu}$ in a magnetic field $\vec{H}$ ($\mu_n = 1.21 \times 10^{-32}$ V sec m),

III is $\vec{E} \times \vec{v}$ term[14] ($\vec{v}$ = velocity of the neutron),

IV is the Foldy term,[15]

V is the intrinsic Foldy term,

VI is the contribution of the polarizability of the neutron [$C_1 = \frac{1}{6} \int r^2 \rho(r) dr$], and

VII is the contribution of the electric dipole moment $\vec{p}$.

Terms II–IV are caused by the magnetic moment $\vec{\mu}_n$. For an unpolarized neutron beam the terms II and III cannot give rise to a shift of the image but only to some broadening. Although the neutron beam was unpolarized it will be shown

that even for a completely polarized beam the deflection is negligible. Interactions V–VII are due to a possible intrinsic structure of the neutron. The effects of terms I–VII are calculated in the Appendix.

VI. POSSIBLE IMPROVEMENTS

It is foreseen that this charge measurement will be repeated in the near future with an improved optical device.

First, the highly chromatic lens will be replaced by a focusing curved mirror. This imaging device is completely achromatic and can therefore make use of the whole spectrum from the neutron guide (10–30 Å). The gain in intensity is expected to be about a factor of 10. The surface of the mirror has to be precise within about 100 Å. If this precision is obtained, a 20-μm-wide entrance slit can be imaged with little broadening of the image. The sensitivity in detecting a deflection will be about five times higher using a curved mirror instead of the quartz lens. In the given set up, the difference in Coriolis deflection for the 10 and 30 Å neutrons is about 25 μm, if the neutrons would travel freely between the slits S_3 and S_4 (Fig. 1). The curved mirror as imaging device corrects this difference in the first approximation, thus the Coriolis force does not lead to a widening of the image.

A further improvement is possible if a large number of slits are imaged instead of a single slit. An optical grating with 20-μm openings and 20-μm-wide absorbing areas could be used. With the given lateral acceptance of the mirror, a 2-mm-wide grating containing 50 slits would be appropriate. A second grating placed in the plane of the image is positioned with its openings on the common side slopes of the 50 images, i.e., 50 slopes are observed simultaneously instead of one.

If imaging is performed by the curved mirror instead of the lens, the electric fields before and behind the mirror have to be arranged in opposite directions. Otherwise, the deflection of a possible charge q_n by the two fields would cancel. Together with a higher electric field (a factor of 2 should be possible), the increase in sensitivity for detecting a deflection—which is proportional to the sensitivity for measuring a possible charge q_n—is expected to be between one and two orders of magnitude. The experimental limit for the charge of the free neutron could then compete with the limits obtained by indirect methods, where the neutrality of molecules or macroscopic bodies is tested.

ACKNOWLEDGMENTS

We would like to express our sincere gratitude to Professor E. Lüscher for the kind hospitality we received in his institute, to the workshop of the Fachbereich Physik of the Technische Universität München for most of the mechanical construction, to the directors and the staff of the ILL for efficient help and worthful discussions, and to Dr. A. Zeilinger for critical reading of the manuscript. This work was supported by the Bundesministerium für Forschung und Technologie.

APPENDIX

It will be proved (see Sec. V) that the deflection of a neutron with a hypothetical charge of $1\times10^{-20}\times q_e$ in the given electric field is large compared with all other deflections caused by the properties of this E field.

Term I

The energy difference due to the hypothetical charge is

$$\Delta Q_{\mathrm{I}} = q_n E_0 \frac{x_0}{2} .$$

For $q_n = 1\times10^{-20}\times1.6\times10^{-19}$ C, $E_0 = 11.9\times10^6$ V/m, and $x_0 = 1$ mm, one gets

$$\Delta Q_{\mathrm{I}} = 9.5\times10^{-36} \text{ J} .$$

Term II

A time-dependent $\vec{E}$ field resulting from the waviness of the HV supply and a leakage current $\vec{j}$ between the electrodes leads to a magnetic field $\vec{H}$. From the Maxwell equation $\vec{H} = \epsilon_0 \delta\vec{E}/\delta t + \vec{j}$ and Stokes law one gets for the leakage current $\vec{j}$

$$\int_a \vec{H}\cdot \vec{dl}_a - \int_b \vec{H}\cdot \vec{dl}_b = \int_F \vec{j}\cdot \vec{df},$$

where F is the area enclosed by the paths a and b. In first approximation $\vec{j}$ is perpendicular to $\vec{df}$ and the integral on the right-hand side becomes zero. Even for $\vec{j}$ parallel to $\vec{df}$ and with the full leakage current (less than 30 μA) passing the area F one gets

$$\Delta Q_{\mathrm{II}} < 3.7\times10^{-38} \text{ J}, \text{ i.e., } \Delta Q_{\mathrm{II}} \ll \Delta Q_{\mathrm{I}} .$$

The waviness of the HV power supply of less than 5×10^{-3} at frequencies of 50 and 100 Hz leads to a current $\epsilon_0 \delta E/\delta t < 170$ μA. Estimated in the same manner as above, the energy difference ΔQ becomes

$\Delta Q_{II} < 2.1 \times 10^{-37}$ J, i.e., $\Delta Q_{II} \ll \Delta Q_I$.

Term III

Owing to the relativistic field equations, a neutron moving with velocity $\vec{v}$ in an $\vec{E}$ field sees a magnetic field $\vec{H}$ with $\vec{H} = (1/\mu_0 c^2)\, \vec{E} \times \vec{v}$. In inhomogeneous $\vec{E}$ fields this gives rise to a force on the magnetic moment of the neutron. The essential inhomogeneities are at the edges of the field plates caused by different lengths of the plates. Along the paths a and b the numbers of field lines crossed by the paths a or b are equal, but the product $\vec{E} \times \vec{v}$ can be bigger for one path, i.e., path a. An upper limit for term III can be derived by taking the maximum value for $\vec{E} \times \vec{v}$ along path a and zero along path b in the region of the inhomogeneous edge fields of length $\Delta l = 2.5$ mm and equal inhomogeneities at two edges. One gets

$$\Delta Q_{III} < \epsilon_0 \vec{\mu} \cdot \vec{E} \times \vec{v} \frac{2\Delta l}{l_0} = 1.3 \times 10^{-36} \text{ J} ,$$

$$\Delta Q_{III} \ll \Delta Q_I .$$

Terms IV and V

According to Foldy,[15] the term IV can be derived from the Dirac equation. It leads to a charge distribution inside the neutron that can be described by two concentric spheres of opposite charge. This charge distribution has zero interaction with an external $\vec{E}$ field, as long as this field shows $\mathrm{div}\vec{E} = 0$. This is true in our case, so terms IV and V are zero.

Terms VI and VII

For the theoretical limits on the polarizability (for example, Ref. 16) and the experimental limit on the dipole moment of the neutron,[17] we note without proof that even in the case $E = 0$ along path a and $E = E_0$ along path b these terms give negligible contributions.

[1] S. L. Glashow, in *Neutrino '79*, proceedings of the International Conference on Neutrinos, Weak Interactions, and Cosmology, Bergen, Norway, 1979, edited by A. Haatuft and C. Jarlskog (University of Bergen, Bergen, 1980), Vol. I, p. 518.

[2] G. Feinberg and M. Goldhaber, Proc. Nat. Acad. Sci. U. S. A. 45, 1301 (1959).

[3] H. F. Dylla and J. G. King, Phys. Rev. A 7, 1224 (1973).

[4] L. G. Chambers, Nature 191, 1082 (1961) and references therein.

[5] V. A. Bailey, J. Proc. R. Soc. N. S. W. 94, 77 (1960) and references therein.

[6] E. D. Garris and K. O. H. Zuck, Nucl. Instrum. Methods 177, 467 (1974).

[7] G. Gallinaro, M. Marinelli, and G. Morpurgo, Phys. Rev. Lett. 38, 1255 (1977).

[8] G. S. LaRue, W. M. Fairbank, and A. F. Hebard, Phys. Rev. Lett. 38, 1011 (1977).

[9] G. S. LaRue, W. M. Fairbank, and J. D. Philipps, Phys. Rev. Lett. 42, 142 (1979).

[10] C. G. Shull, K. W. Billmann, and F. A. Wedgwood, Phys. Rev. 153, 1415 (1967).

[11] R. Gähler, J. Kalus, and W. Mampe, J. Phys. E 13, 546 (1980).

[12] R. A. Fisher, *Statistical Methods for Research Works* (Oliver and Boyd, Edinburgh/London, 1958).

[13] H. Rauch, *Neutron Interferometry*, edited by U. Bonse and H. Rauch (Oxford University Press, New York, 1979), p. 161.

[14] J. Schwinger, Phys. Rev. 69, 681 (1948).

[15] L. L. Foldy, Rev. Mod. Phys. 30, 471 (1958).

[16] G. Dattoli, G. Matone, and D. Prosperi, Lett. Nuovo Cimento 19, 601 (1977).

[17] W. B. Dress, P. D. Miller, J. M. Pendlebury, P. Perrin, and N. F. Ramsey, Phys. Rev. D 15, 9 (1977).